JOURNAL OF GEOPHYSICAL RESEARCH, VOL. 100, NO. D6, PAGES 11,641–11,660, JUNE 20, 1995

Two-dimensional and three-dimensional model simulations, measurements, and interpretation of the influence of the October 1989 solar proton events on the middle atmosphere

Charles H. Jackman,[1] Mark C. Cerniglia,[2] J. Eric Nielsen,[2] Dale J. Allen,[2] Joseph M. Zawodny,[3] Richard D. McPeters,[1] Anne R. Douglass,[1] Joan E. Rosenfield,[2] and Richard B. Rood[1]

Abstract. The very large solar proton events (SPEs) which occurred from October 19 to 27, 1989, caused substantial middle-atmospheric HO_x and NO_x constituent increases. Although no measurements of HO_x increases were made during these SPEs, increases in NO were observed by rocket instruments which are in good agreement with calculated NO increases from our proton energy degradation code. Both the HO_x and the NO_x increases can cause ozone decreases; however, the HO_x-induced ozone changes are relatively short-lived because HO_x species have lifetimes of only hours in the middle atmosphere. Our two-dimensional model, when used to simulate effects of the longer-lived NO_x, predicted lower-stratospheric polar ozone decreases of greater than 2% persisting for one and a half years past these SPEs. Previous three-dimensional model simulations of these SPEs (Jackman et al., 1993) indicated the importance of properly representing the polar vortices and warming events when accounting for the ozone decreases observed by the solar backscattered ultraviolet 2 instrument two months past these atmospheric perturbations. In an expansion of that study, we found that it was necessary to simulate the November 1, 1989, to April 2, 1990, time period and the November 1, 1986, to April 2, 1987, time period with our three-dimensional model in order to more directly compare to the stratospheric aerosol and gas experiment (SAGE) II observations of lower stratospheric NO_2 and ozone changes between the end of March 1987 and 1990 at 70°N. Both the NO_x increases from the October 1989 SPEs and the larger downward transport in the 1989-1990 northern winter compared to the 1986-1987 northern winter contributed to the large enhancements in NO_2 in the lower stratosphere observed in the SAGE II measurements at the end of March 1990. Our three-dimensional model simulations predict smaller ozone decreases than those observed by SAGE II in the lower stratosphere near the end of March 1990, indicating that other factors, such as heterogeneous chemistry, might also be influencing the constituents of this region.

[1]Laboratory for Atmospheres, NASA Goddard Space Flight Center, Greenbelt, Maryland.
[2]Applied Research Corporation, Landover, Maryland.
[3]Atmospheric Sciences Division, NASA Langley Research Center, Hampton, Virginia.

Paper number 95JD00369.
0148-0227/95/95JD-00369$05.00

1. Introduction

Solar proton events (SPEs) have been associated with significant ozone loss during several periods over the past 20 years [e.g., *Weeks et al.*, 1972; *Heath et al.*, 1977; *McPeters et al.*, 1981; *Thomas et al.*, 1983; *Solomon et al.*, 1983; *McPeters and Jackman*, 1985]. The primary cause of the ozone depletion observed in most of these SPEs is thought to be the HO_x (H, OH, HO_2) production during the SPEs. The HO_x-

induced ozone depletions are confined to the mesosphere and upper stratosphere and are relatively short-lived, since HO_x lifetimes and ozone recovery times in this region are only of the order of hours. The only events in the 1963-1984 time period (solar cycles 20 and 21) that created enough NO_x (N, NO, NO_2) to cause a significant ozone depletion in the middle to upper stratosphere were the August 1972 SPEs [e.g., *Crutzen et al.*, 1975; *Solomon and Crutzen*, 1981; *Reagan et al.*, 1981; *Rusch et al.*, 1981; *Jackman et al.*, 1990].

The latest solar cycle has been quite active. In 1989 alone, large SPEs were recorded in the months of March, August, September, and October. The most significant SPEs of solar cycle 22 occurred from October 19 to 27, 1989. The HO_x and NO_x increases which resulted from these SPEs were predicted to lead to >20% depletions in upper stratospheric ozone at polar latitudes using two-dimensional and three-dimensional models [*Reid et al.*, 1991; *Jackman*, 1993; *Jackman et al.*, 1993]. The ozone depletion is predicted to be prolonged for over a year following these SPEs by the transport of the long-lived NO_x constituents to the middle and lower stratosphere [*Jackman*, 1993]. Commensurate with these predictions were measurements of enhanced NO from a rocket-borne instrument [*Zadorozhny et al.*, 1992] and of reduced ozone from a satellite instrument [*Jackman et al.*, 1993] during and after the October 1989 SPEs.

Quantifying the effects of SPEs on the middle atmosphere is relatively straightforward during and soon after the events, however, the longer-term influences (approximately months after the SPEs) are often quite difficult to quantify. Seasonal changes driven by solar forcing and dynamical variations intermix with the SPE-induced atmospheric anomalies. We have used both two-dimensional and three-dimensional photochemical transport models to assess the response of the middle atmosphere to these external influences on time periods of weeks to years past the SPEs. The two-dimensional model has enabled us to remove the interference caused by solar-forced changes (change of Sun angle over the different seasons) and has given us insight into some of the expected dynamical variations. The three-dimensional model helped us to simulate more realistically the interhemispheric dynamical differences in the work of *Jackman et al.* [1993] and has made it possible here to quantify the dynamical variations that influence some of the changes observed in stratospheric aerosol and gas experiment (SAGE) II data when 2 years of measurements are compared with one another.

We have computed the influence of the October 1989 SPEs on the lower stratosphere five months past these events which initially perturbed the upper stratosphere. We have also quantified some of the large interannual constituent changes at northern polar latitudes expected between early spring 1987 and early spring 1990 caused by the large differences in wintertime downward transport between the two years.

We will present the following: a discussion of the SPE production of NO_x and HO_x (section 2), a description of the photochemical transport models employed in this study (section 3), the differences of the ozone response in each hemisphere caused by the October 1989 SPEs (section 4), the predicted temperature change associated with the October 1989 SPEs (section 5), evidence (both measurements and simulations) for substantial downward transport in the northern polar winter of December 1989 to March 1990 (section 6), and conclusions (section 7).

2. Proton Flux Data: SPE Production of NO_x and HO_x

Proton fluxes from T. Armstrong and colleagues (University of Kansas, private communication, 1991) allow for daily computation of ion pair production and NO_x production due to SPEs in 1989. These fluxes were measured on the IMP 8 satellite and are given in daily average differential form (units are cm^{-2} s^{-1} sr^{-1} MeV^{-1}) for the 10 energy bins (in megaelectron volts, MeV): (1) 0.29 to 0.5, (2) 0.5 to 0.96, (3) 0.96 to 2.0, (4) 2.0 to 4.6, (5) 4.6 to 15.0, (6) 15.0 to 25.0, (7) 25.0 to 48.0, (8) 48.0 to 96.0, (9) 96.0 to 145.0, and (10) 190.0 to 440.0. We have derived differential proton spectra from these data by fitting the proton data from T. Armstrong with an empirical formula of a power law form for several intervals:

$$\Phi(E) = dF/dE = A_o (E/E_o)^{-n} \text{ cm}^{-2} \text{ s}^{-1} \text{ sr}^{-1} \text{ MeV}^{-1}$$

where $\Phi(E)$ is the proton differential flux, E is the proton energy in MeV, F is the proton integral flux, A_o and n are parameters, and E_o is simply set to 1 MeV. The five intervals were (in MeV): (1) 0.29 to 0.96, (2) 0.96 to 4.6, (3) 4.6 to 25.0, (4) 25.0 to 96.0, and (5) 96.0 to 440.0.

The flux of protons, $\Phi(E)$, at the top of the atmosphere is divided up into 60 monoenergetic energy intervals. Each of these monoenergetic proton fluxes were assumed to be isotropic and were degraded in energy following *Jackman et al.* [1980] to give a daily average ion pair production profile.

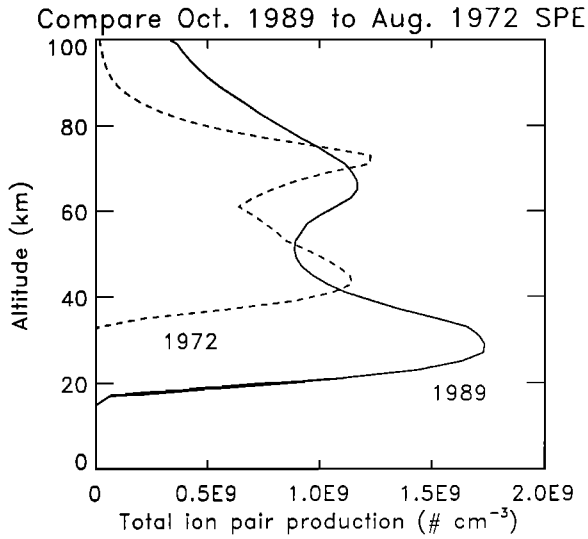

Figure 1. Total computed ion pair production (in number of ion pairs per cm^3) for the August 1972 and October 1989 solar proton events.

We added up the ion pair production during the October 1989 SPEs and compared it to that computed for the August 1972 SPEs, since these are two of the largest SPE periods of the past two solar cycles. These calculations of total ion pair production are shown in Figure 1. The ion pair production during the October 1989 SPEs is larger than the August 1972 SPEs except in two altitude intervals (42-52 and 70-76 km). The October 1989 SPEs have a substantially larger ion pair production than the August 1972 SPEs in the lower stratosphere. Most of this difference is probably due to the fact that the ion pair production for the August 1972 SPEs was computed using an artificial cutoff for the proton energy of 100 MeV (required when using the proton flux data set of *Armstrong et al.* [1983] and the Solar Geophysical Data publication), whereas the ion pair production for the October 1989 SPEs was computed with a cutoff for the proton energy of 440 MeV. The 1972 SPEs probably did have protons with energies above 100 MeV, but these were not accounted for in the data set used by *Jackman et al.* [1990].

The SPE-produced HO_x was included in our two-dimensional model simulation in the following ways: (1) below 70 km, each ion pair was assumed to result in the formation of two HO_x species; and (2) above 70 km the HO_x species production per ion pair was taken from *Solomon et al.* [1981, Figure 2]. Since the HO_x produced by SPEs lasts only hours after the events have abated (short-lived) and since we are interested in the longer-term ozone influence by the October 1989 SPEs, we only considered the longer-lived NO_x produced by the SPEs in our three-dimensional model simulations.

We assume that 1.25 N atoms are produced per ion pair. This is similar to the value given by *Porter et al.* [1976], which was derived using a detailed theoretical energy degradation computation. The protons are assumed to enter the atmosphere uniformly for latitudes ≥60° geomagnetic. Few measurements exist for NO production from SPEs. We found relatively good agreement between our NO production computed from the July 1982 SPE compared to solar backscattered ultraviolet (SBUV) measurements in the work of Jackman et al. [1990]. Using our computed production of N atoms and assuming that they all result in a production of NO by the $N + O_2 \rightarrow NO + O$ reaction with no production of other odd nitrogen constituents, such as NO_2, we compute an NO increase over the 50- to 90-km altitude range of 3.0×10^{15} molecules cm^{-2} from October 19 to 23, 1989. *Zadorozhny et al.* [1992] measured NO enhancements of 2.6×10^{15} molecules cm^{-2} between 50 and 90 km at southern polar latitudes using a rocket-borne instrument during the same time period. Our computation results in an overprediction of NO because some of the NO_x is destroyed through the reaction $N + NO \rightarrow N_2 + O$. However, our calculation gives a reasonable upper limit of NO_x in the southern hemisphere between 50 and 90 km, where almost all of it is in the form of NO.

3. Models Description

3.1. Two-Dimensional Model

The two-dimensional model of stratospheric photochemistry and dynamics used in this study is described by *Douglass et al.* [1989] and *Jackman et al.* [1990]. Its vertical range, equally spaced in log pressure, is from the ground to approximately 90 km (0.0024 hPa) with approximately a 2-km grid spacing. Latitudes range from 85°S to 85°N with a 10° grid spacing. Forty-six individual constituents are considered, including those comprising the O_x, NO_y, HO_x, Cl_y, and Br_y families. The 130 chemical reactions included are as specified by *DeMore et al.* [1990].

Twenty-two species or families (O_x, NO_y, Cl_y, and Br_y) are transported in the model simulations used here. These include O_x (O_3, $O(^1D)$, $O(^3P)$), NO_y (N, NO, NO_2, NO_3, N_2O_5, HO_2NO_2, $ClONO_2$, but not including HNO_3), Cl_y (Cl, ClO, HOCl, HCl, $ClONO_2$), Br_y (Br, BrO, HBr, $BrONO_2$), HNO_3, N_2O, CH_4, H_2, CO, CH_3OOH, $CFCl_3$, CF_2Cl_2, CH_3Cl, CCl_4, CH_3CCl_3, CH_3Br, $CHClF_2$, $C_2Cl_3F_3$, $C_2Cl_2F_4$, C_2ClF_5, $CBrClF_2$, and $CBrF_3$. The HO_x (H, OH,

HO_2) species, H_2O_2, and the hydrocarbons CH_3, CH_3O, CH_3O_2, CH_2O, and CHO are calculated using photochemical equilibrium assumptions. The CO_2 mixing ratio is set at 330 ppmv and the H_2O distribution is fixed using limb infrared monitor of the stratosphere (LIMS) measurements and other model calculations described by *Jackman et al.* [1987]. Ground boundary conditions for the trace gases are taken from *World Meteorological Organization* (*WMO*) [1992, Table 8-6b] for the 1990 steady state. The residual circulation and diffusion specification is the dynamics A formulation described by *Jackman et al.* [1991], with the exception of the horizontal eddy diffusion coefficients (K_{yy}s). The K_{yy}s are computed to be consistent with the circulation as described by *Fleming et al.* [1995].

3.2. Two-Dimensional Model Simulations

We investigated the effect of the SPEs in two sets of simulations. One set of simulations, called the "gas phase only" runs, included only gas phase chemistry. The other set of simulations, called the "gas phase + het" runs, included the heterogeneous processes of $N_2O_5 + H_2O \rightarrow 2HNO_3$ and $ClONO_2 + H_2O \rightarrow HOCl + HNO_3$ on the background sulfate aerosol layer that have been shown to be important when simulating processes in the lower stratosphere [see *Weisenstein et al.*, 1991; *WMO*, 1992]. The surface area of aerosols specified in *WMO* [1992] was used in the "gas phase + het" runs. It is thought that the "gas phase + het" run is more realistic when dealing with the tropics, midlatitudes, and southern polar latitudes. The "gas phase only" simulations should be closer to the real atmosphere for the lower northern polar stratosphere in the early spring period. The very large downward transport should convey air from the upper stratosphere, which is relatively clean of aerosols, throughout the 1989-1990 winter period.

Our two-dimensional model was run for 20 years to a steady-state annually repeating cycle to establish the model atmospheric condition for 1990 in both the "gas phase only" and the "gas phase + het" modes. We then completed four separate 4-year runs starting from January 1, 1989: (1) A base "gas phase only" run with no SPEs included; (2) a perturbed "gas phase only" run with all SPEs in 1989 included; (3) a base "gas phase + het" run with no SPEs included; and (4) a perturbed "gas phase + het" run with all SPEs in 1989 included. The second run was then compared to the first for the "gas phase only" condition and the fourth run was then compared to the third for the "gas phase + het" condition.

Our computations of NO_y and the associated ozone percentage change at 75°N and 75°S due to the 1989 SPEs are presented in Figure 2 for 3 years. Results from both the "gas phase only" and the "gas phase + het" model simulations are presented in this figure. The changes are largest in the upper stratosphere and lower mesosphere for both hemispheres. Transport of the NO_y carries enhancements to lower altitudes over the next couple of years. The computed increases in NO_y for both the "gas phase only" and the "gas phase + het" modes are nearly the same. The computed decreases in O_3 are different in the two model modes below about 10 hPa (~30 km): the "gas phase only" simulations produce a larger ozone decrease due to the SPEs, as a result of a larger fraction of the NO_y being in the reactive NO_x species, than is indicated in the "gas phase + het" simulations. The increases in NO_y of several percent and associated decreases in ozone of greater than 2% persist for about a year and a half after the extremely intense October 1989 SPEs in both sets of simulations.

Our results are similar to those reported by *Reid et al.* [1991]. It does appear that our results indicate more downward transport at northern polar latitudes than computed by *Reid et al.* [1991]. The downward transport of NO_2 during the northern polar winter will be examined in more detail in section 5 when our model results are compared with SAGE II measurements.

We find the largest simulated changes in total ozone in 1990 as a result of the 1989 SPEs (see Figure 3). We only present the "gas phase + het" model in this figure, because this mode is thought to be more realistic over the entire model domain than is the "gas phase only" model mode. The largest depletions (>4%) are predicted to occur near the pole in the northern hemisphere summer. Because of the large variation in total ozone on all timescales from weeks to years at the high latitudes, it would be unlikely that such SPE-related changes in total ozone could be measured unambiguously.

3.3. Three-Dimensional Models

Winds and temperatures for the three-dimensional chemistry and transport simulation are generated by a global spectral mechanistic model (GSMM). The formulation and performance of the GSMM is described by *Nielsen et al.* [1994]. The lower boundary lies at 100 hPa and is specified with observed geopotentials as the integration proceeds. The planetary waves thus evolve as observed in the lower stratosphere and freely interact as they vertically propagate. Local heating rates are provided by

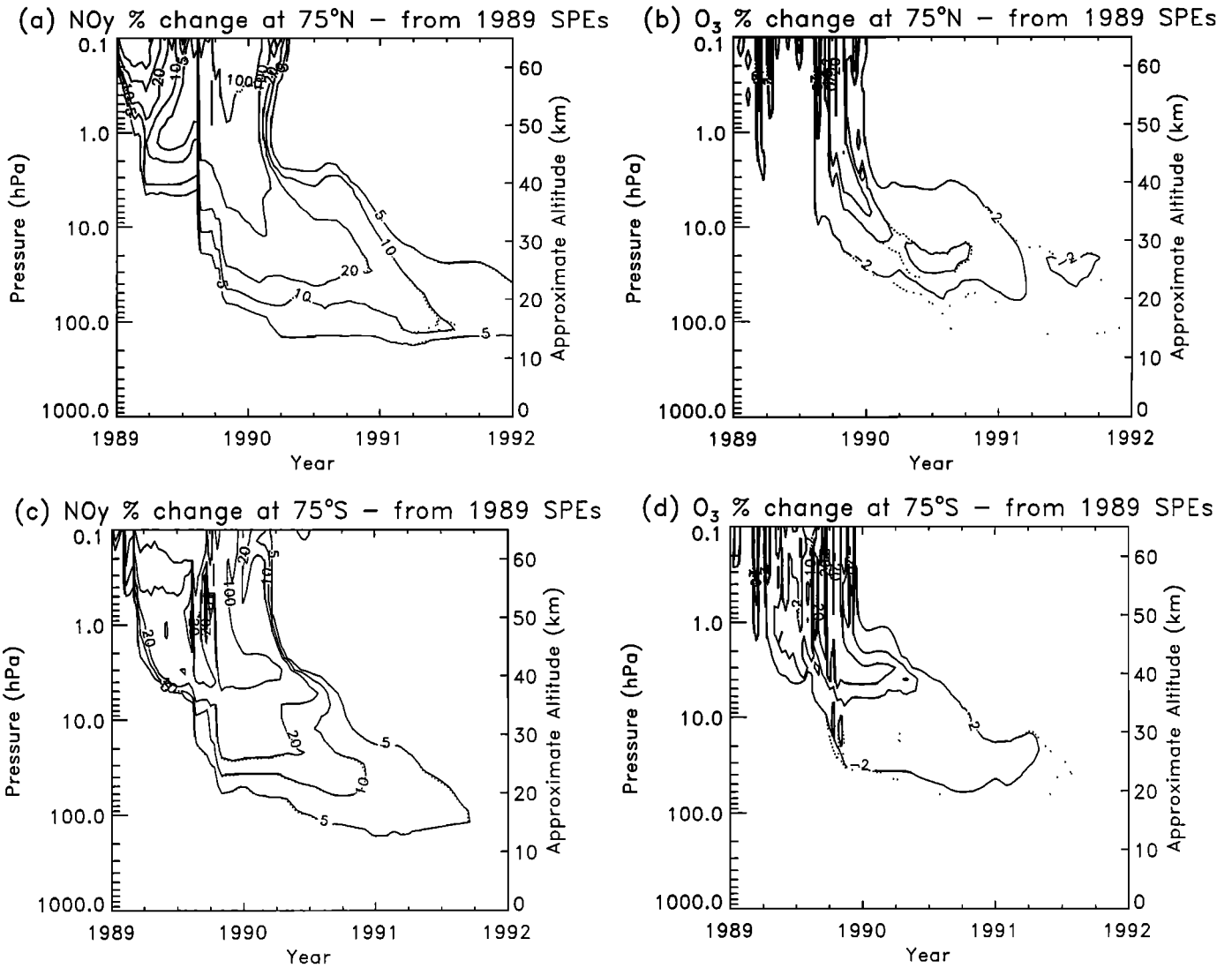

Figure 2. Goddard Space Flight Center (GSFC) two-dimensional model-calculated percentage changes in (a) NO_y at 75°N, (b) O_3 at 75°N, (c) NO_y at 75°S, and (d) O_3 at 75°S resulting from solar proton events in 1989 for 3 years starting from January 1, 1989. Contour intervals for NO_y are 5, 10, 20, 100, and 1000%. Contour intervals for O_3 are -2, -10, and -20%. The solid and the dotted curves indicate percentage changes from the "gas phase + het" and the "gas phase only" simulations, respectively.

an accurate radiative transfer algorithm, and momentum dissipation is parameterized through a vertically and latitudinally dependent Rayleigh friction.

The three-dimensional chemistry and transport model (CTM) is described by *Allen et al.* [1991] and *Rood et al.* [1992]. It operates off-line from the GSMM. Six-hourly time averaged GSMM temperatures and horizontal wind components are interpolated onto the CTM's staggered horizontal grid. Vertical winds are calculated internally by the kinematic method. Upstream biased techniques are used to solve the constituent continuity equation. The vertical discretization, 30 levels, is identical to that in the GSMM, with the domain ranging from 100 to 0.01 hPa. The horizontal resolution, 80 longitudes on 65 latitudes, closely approximates that of the GSMM's Gaussian grid.

For the SPE experiments, simplified homogeneous photochemistry is used in the CTM which includes fairly complete O_x, NO_y, HO_x, and Cl_y chemistry. Nineteen minor constituents (O_3, O, $O(^1D)$, N, NO, NO_2, NO_3, N_2O_5, HNO_3, HO_2NO_2, H, OH, HO_2, H_2O_2, $ClONO_2$, Cl, ClO, HCl, and HOCl) are calculated in the model with 10 constituents/families being transported. The transported constituents include (1) O_x (O_3, O, $O(^1D)$), (2) NO_x (N, NO, NO_2, NO_3), (3) N_2O_5, (4) HNO_3, (5) HO_2NO_2, (6) H_2O_2, (7) $ClONO_2$, (8) Cl_x (Cl, ClO), (9) HCl, and

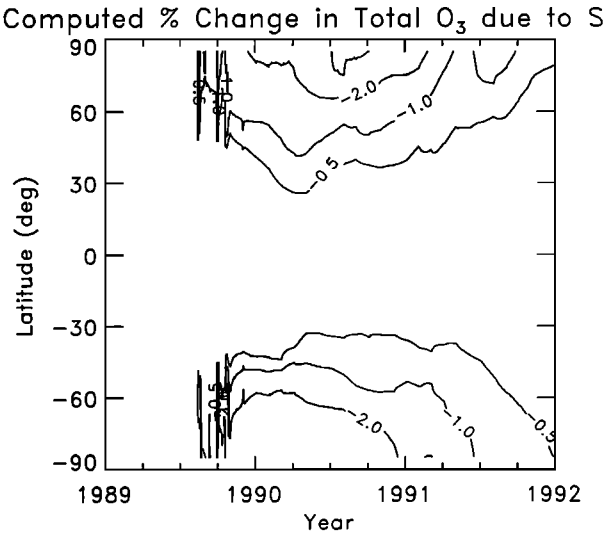

Figure 3. GSFC two-dimensional model "gas phase + het" computed percentage total ozone changes in 1989, 1990, and 1991 which resulted from solar proton events in 1989. Contour intervals are -0.5, -1, -2, and -4%.

(10) HOCl. The HO_x (H, OH, and HO_2) species are calculated using photochemical equilibrium assumptions. The stratospheric and mesospheric H_2O distribution is fixed to LIMS measurements where possible and is explained by *Jackman et al.* [1987]. The N_2O, CH_4, and Cl_y (Cl, ClO, $ClONO_2$, HCl, and HOCl) distributions are taken from a two-dimensional model simulation of October 23, 1989, to April 2, 1990. We omitted bromine chemistry from these CTM studies due to computational constraints. Reactions involving bromine species are of minimal importance to this study.

We use "gas phase only" chemistry in our three-dimensional model simulations. We analyze the 10.8-hPa surface and the lower northern polar stratosphere in the early spring period in great detail from our three-dimensional model. These regions should be fairly well represented by "gas phase only" chemistry (also, see discussion in section 3.2).

3.4. Three-Dimensional Model Simulations

The GSMM was initialized on October 23, 1989, with gradient balanced National Meteorological Center (NMC) observations at pressures greater than 0.40 hPa and with zonally averaged climatology at lower pressures. After approximately nine days the planetary waves propagate into the mesosphere and the initial dynamical inconsistencies in the tropics become negligible. Thus winds are suitable for transport beginning November 1, 1989. Both the "1989-1990 base run" and the "1989-1990 SPE run" use these winds as starting conditions and the GSMM is run through the following 5 months until April 2, 1990.

A similar method is applied in the simulation for the "1986-1987 base run." The GSMM is initialized on October 23, 1986, as described above and is run for 9 days up to November 1, 1986. The "1986-1987 base run" uses these winds as starting conditions and the GSMM is run through the following 5 months until April 2, 1987.

Three chemistry and transport model simulations were completed in this study: (1) a November 1, 1989, to April 2, 1990, base run ("1989-1990 base run"); (2) a November 1, 1989, to April 2, 1990, SPE run ("1989-1990 SPE run"); and (3) a November 1, 1986, to April 2, 1987, base run ("1986-1987 base run"). These model experiments allowed us to investigate the effects of the SPEs on the background atmosphere as well as the differences caused by dynamical variations between the 1986-1987 and the 1989-1990 November through April time periods.

We initialize constituents for the three model simulations in the following way: Constituent fields from the two-dimensional model are mapped onto the three-dimensional CTM grid by utilizing the dynamical balancing scheme described by *Lary et al.* [1994]. The method assumes that potential vorticity acts as a conservative tracer and under adiabatic conditions the constituents are transported on isentropic surfaces. From the GSMM data sets, a potential vorticity equivalent latitude (horizontal) and potential temperature (vertical) vortex-centered coordinate system is defined. The two-dimensional model constituent fields are mapped onto the global coordinates using bilinear interpolation in this regime. Potential vorticity equivalent latitude is determined at each three-dimensional CTM grid point by calculating the area enclosed by a given isentropic potential vorticity contour and is set equal to the latitude of the latitude circle which occupies that area. The two-dimensional model latitudes serve as the two-dimensional potential vorticity equivalent latitudes. This method of tracer initialization reduces the time required for the starting conditions to reach dynamical and chemical equilibrium with the present state of the atmosphere.

The "1989-1990 SPE run" initial condition was identical to the "1989-1990 base run," except that the November 1, 1989, model output from the two-dimensional calculation with SPEs was used to initialize NO_y. SPEs affect regions of the Earth's atmosphere poleward of approximately geomagnetic latitude 60°, therefore NO_y was increased at the grid points in these polar regions.

The November 1, 1989, orthographic polar projections of NO_y enhancement for the northern hemisphere (Plate 1a) and for the southern hemisphere

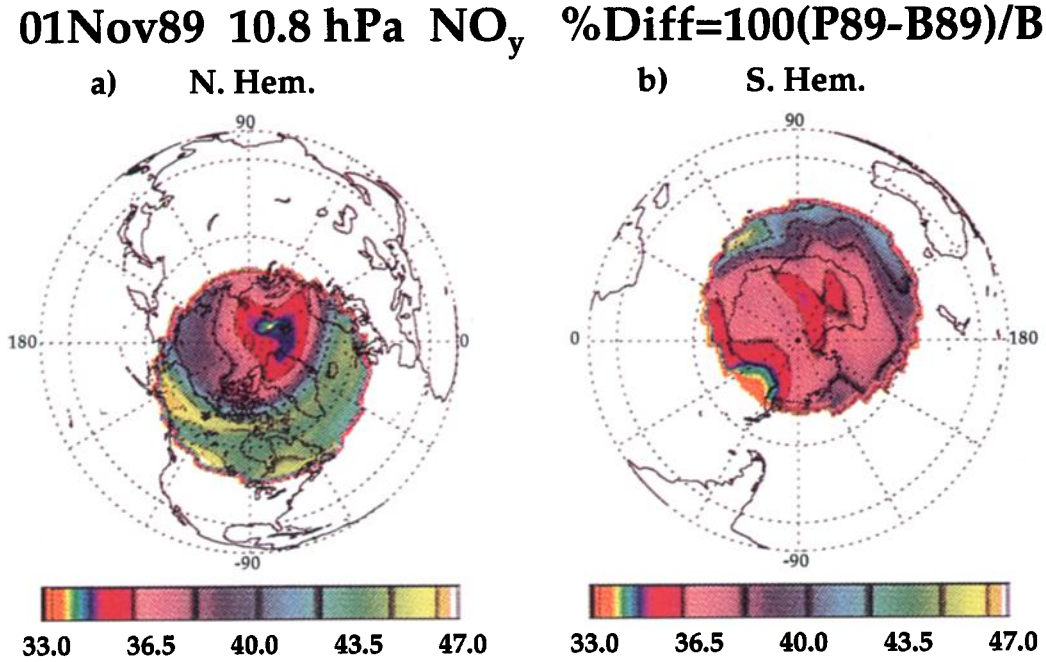

Plate 1. Initial conditions of NO_y percentage difference when comparing the "1989-1990 SPE run" to the "1989-1990 base run" from the GSFC three-dimensional model for the (a) northern hemisphere (NH) and (b) the southern hemisphere (SH) at 10.8 hPa on November 1, 1989. The percentage difference (%diff) is computed by subtracting the "1989-1990 base run" (B89) from the "1989-1990 SPE run" (P89), dividing that difference by the "1989-1990 base run" (B89), and multiplying the result by 100.

(Plate 1b) show starting conditions for the three-dimensional perturbed run at 10.8 hPa. The inter-hemispheric differences in percentage enhancement of NO_y is mainly caused by the dissimilar background NO_y amounts in the two polar regions and not by the absolute quantity of NO_y increase, which is nearly the same in both hemispheres.

4. Interhemispheric Differences in Ozone Depletion Following the October 1989 SPEs

Jackman et al. [1993] focused attention on three-dimensional model simulations at the 4.18-hPa surface. Since we show simulations over a longer time period than indicated in that work (5 months versus 2 months) with downward transport becoming increasingly important, we illustrate the NO_y and O_3 changes at 10.8 hPa in Plates 2-5, expanding our previous analysis [*Jackman et al.*, 1993]. We only compare the "1989-1990 SPE run" with the "1989-1990 base run" in this section. Plates 2 and 3 orthographic polar projections show predicted percentage change in northern hemispheric NO_y and O_3 resulting from the October 1989 SPEs for days November 5, and December 1 and 31, 1989, and for days February 1, March 1, and April 1, 1990. Plates 4 and 5 show predicted percentage change in southern hemispheric NO_y and O_3 resulting from the October 1989 SPEs for the same days as in Plates 2 and 3. Hereafter, the percentage changes in NO_y and O_3 will be referred to as $p(NO_y)$ and $p(O_3)$, respectively.

In the northern hemisphere the initial SPE perturbation is "instantaneously injected" into the developing winter polar vortex and is rapidly distorted (Plates 2a and 2b). During November, however, the NO_y perturbation takes on the characteristics of the wind field, and by December 1, 1989, its configuration at 10.8 hPa clearly outlines the polar vortex (Plate 2c). Ozone loss is controlled by the catalytic cycle

$$NO + O_3 \rightarrow NO_2 + O_2$$
$$NO_2 + O \rightarrow NO + O_2$$
$$\text{Net: } O_3 + O \rightarrow O_2 + O_2$$

and the required atomic oxygen is formed only in the presence of sunlight. Without sunlight, there is no mechanism for NO_y to directly affect O_3; that is, O_3 depletion due to NO_y enhancement will occur only in parcels which periodically flow in and out of the expanding darkness of polar night. O_3 loss generally occurs at less than Arctic latitudes, often near the edge of the polar vortex, and away from the region which has the largest NO_y perturbation (Plates 2b and 2d).

By the end of December, however, the correlation between enhanced NO_y and depleted O_3 is high. It is most likely due to the isolated nature of vortical

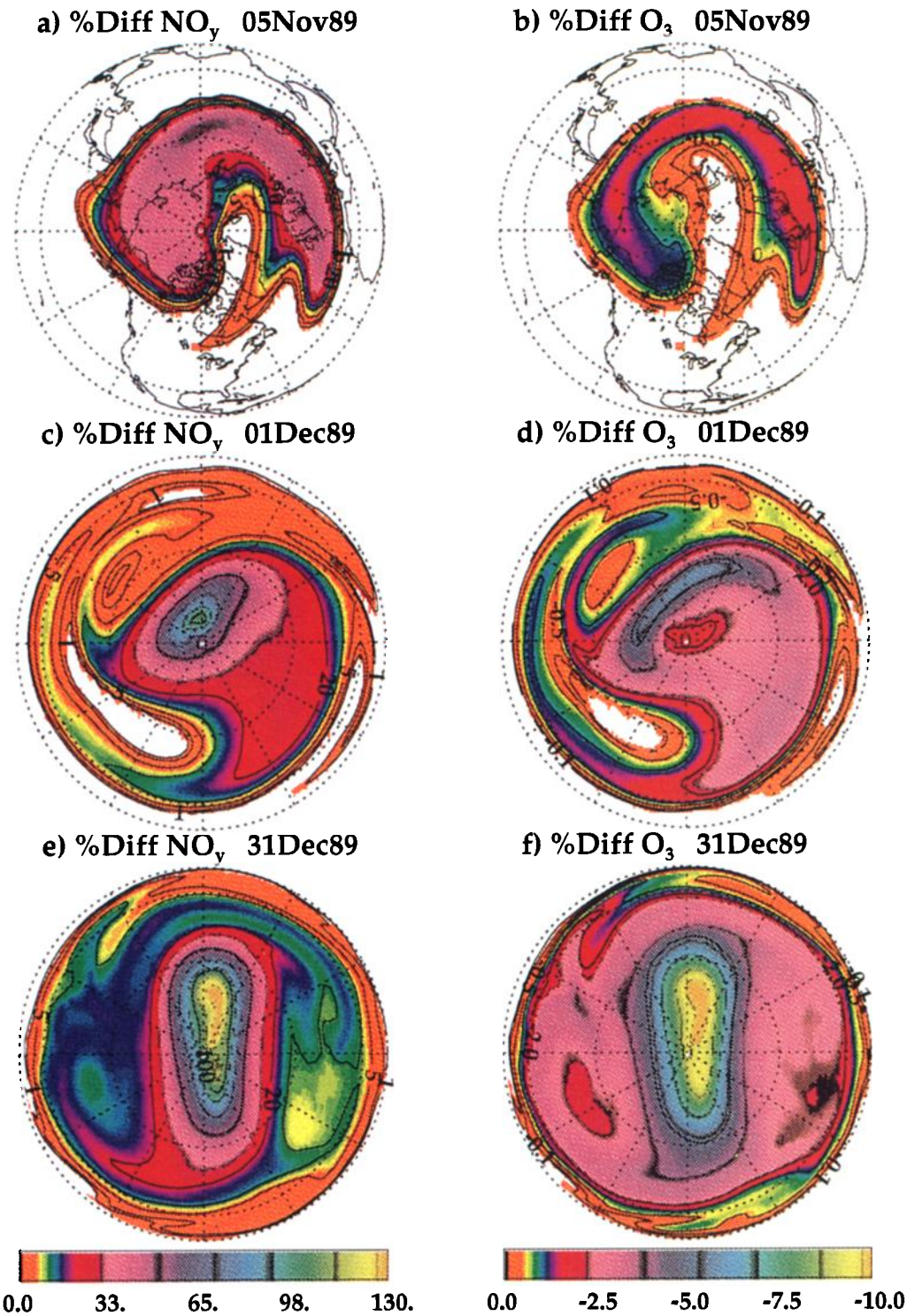

Plate 2. (a, c, and e) NH NO_y. (b, d, and f) NH O_3 percentage difference predicted when comparing the "1989-1990 SPE run" to the "1989-1990 base run" from the GSFC three-dimensional model for November 5, 1989; December 1, 1989; and December 31, 1989 at 10.8 hPa. The percentage difference (%diff) is computed by subtracting the "1989-1990 base run" (B89) from the "1989-1990 SPE run" (P89), dividing that difference by the "1989-1990 base run" (B89), and multiplying the result by 100.

air. The vortex during the last two months of 1989 is temporarily pushed well off the pole by two moderately large planetary wave events. In each case, the vortex moves toward sunlight, O_3 depletion occurs, and the winds then act to homogeneously mix the perturbation within the containment of the vortex. By the end of the year the $p(NO_y)$ and $p(O_3)$ clearly outlines the mature polar vortex (Plates 2e and 2f).

Despite large planetary wave amplitudes during

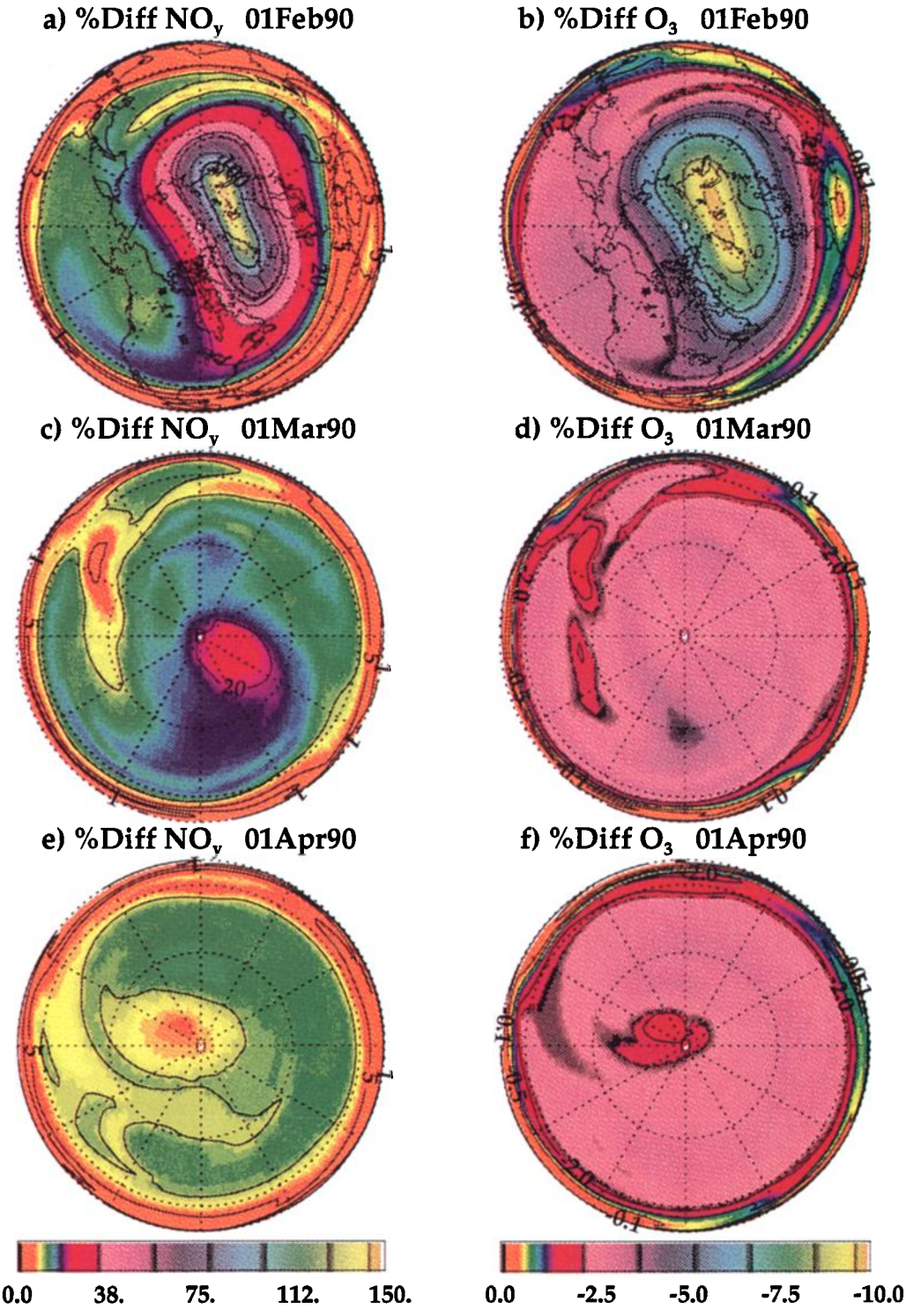

Plate 3. (a, c, and e) NH NO_y. (b, d, and f) NH O_3 percentage difference predicted when comparing the "1989-1990 SPE run" to the "1989-1990 base run" from the GSFC three-dimensional model for February 1, 1990; March 1, 1990; and April 1, 1990 at 10.8 hPa. The percentage difference (%diff) is computed by subtracting the "1989-1990 base run" (B90) from the "1989-1990 SPE run" (P90), dividing that difference by the "1989-1990 base run" (B90), and multiplying the result by 100.

January the chemical perturbations remain intact and at 10 hPa on February 1, 1990 still reflect the position of the vortex, which is slightly displaced from the pole (Plates 3a and 3b). While the $p(O_3)$ has remained about constant, $p(NO_y)$ has increased. This is a reminder that downward transport of the perturbations is also an important consideration. Despite the occurrence of a major warming in

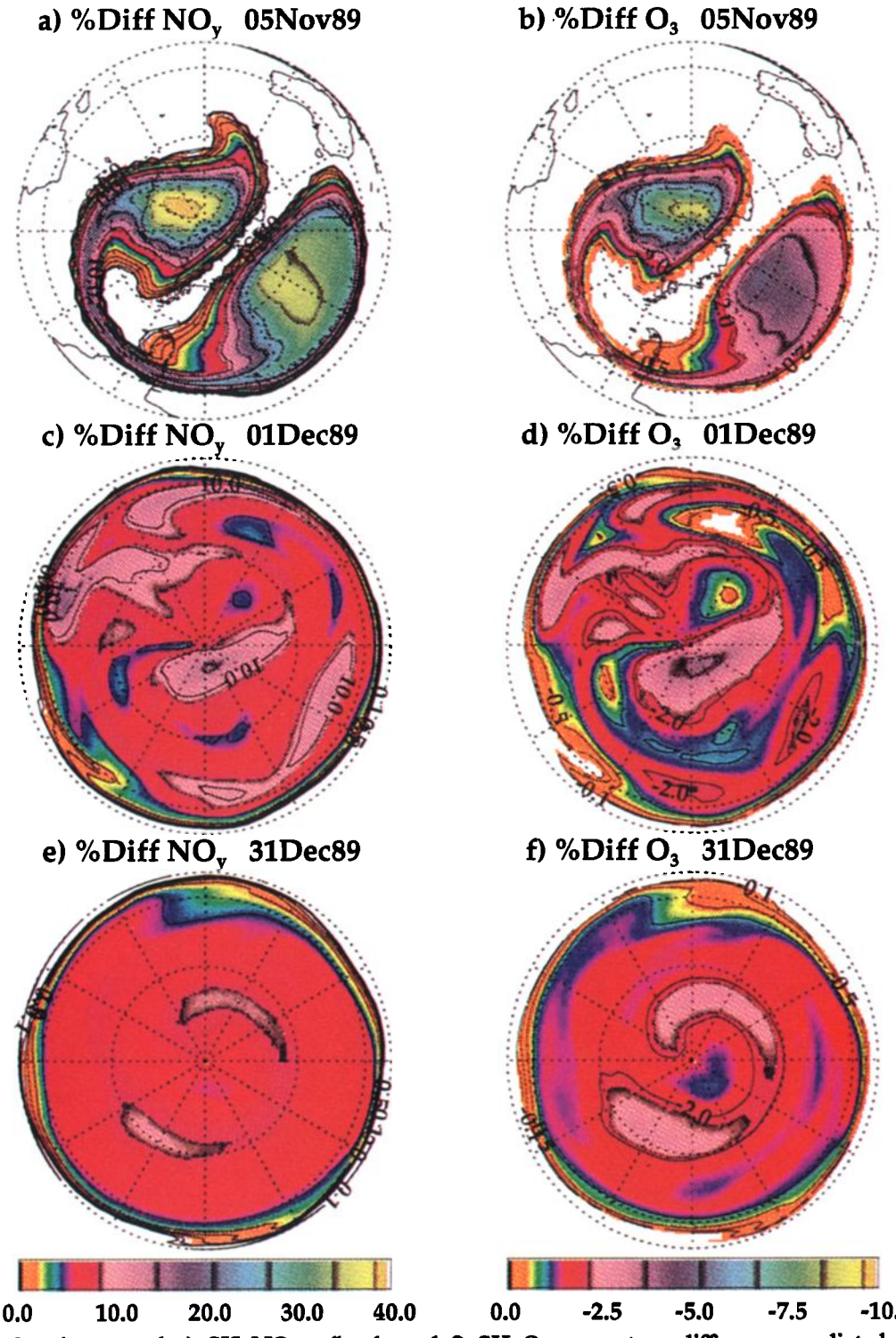

Plate 4. (a, c, and e) SH NO_y. (b, d, and f) SH O_3 percentage difference predicted when comparing the "1989-1990 SPE run" to the "1989-1990 base run" from the GSFC three-dimensional model for November 5, 1989, December 1, 1989, and December 31, 1989, at 10.8 hPa. The percentage difference (%diff) is computed by subtracting the "1989-1990 base run" (B89) from the "1989-1990 SPE run" (P89), dividing that difference by the "1989-1990 base run" (B89), and multiplying the result by 100.

February, in which some material must be ejected from the vortex, the primary reason for large reductions in $p(O_3)$ and $p(NO_y)$ (see Plates 3c-3f) is that the center of mass of the remnants of the perturbations descend to higher pressures. Polar descent is more extensively discussed in section 6.

Over the south pole, at the time of the SPEs, the circulation in the stratosphere is making a transition

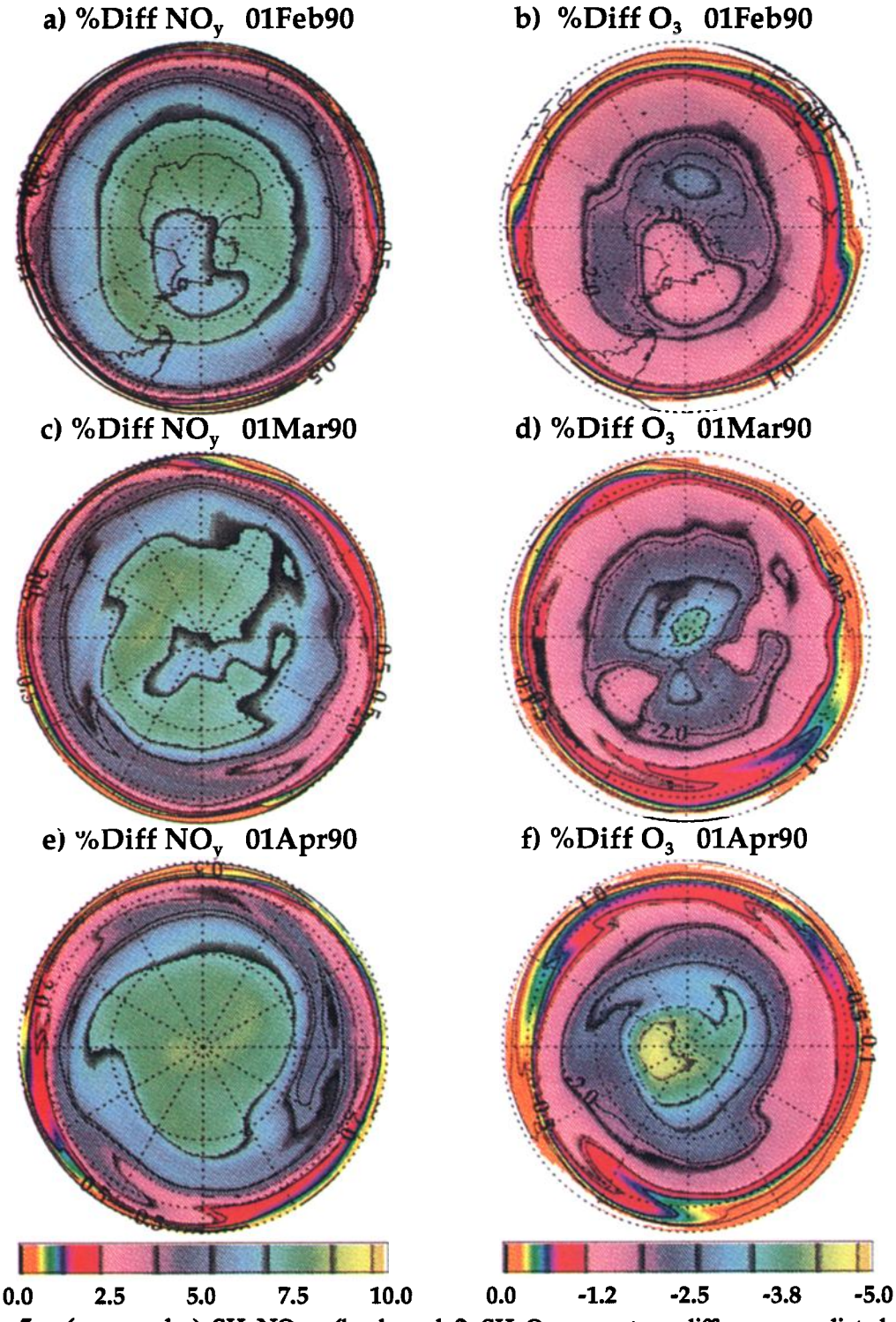

Plate 5. (a, c, and e) SH NO_y. (b, d, and f) SH O_3 percentage difference predicted when comparing the "1989-1990 SPE run" to the "1989-1990 base run" from the GSFC three-dimensional model for February 1, 1990, March 1, 1990, and April 1, 1990 at 10.8 hPa. The percentage difference (%diff) is computed by subtracting the "1989-1990 base run" (B90) from the "1989-1990 SPE run" (P90), dividing that difference by the "1989-1990 base run" (B90), and multiplying the result by 100.

from winter to summer. The NO_y perturbation is thus "injected" into a highly sheared wind field, characteristic of several vortices of decreasing vertical extent. In fact, Plates 4a and 4b show that the initial perturbation is immediately split into two distinct centers. Despite such rapid deformation the ozone depletions are immediately highly correlated with the NO_y enhancements. Since the Sun has

risen on the pole, the catalytic cycle described above acts to keep the correlation high throughout the model experiment.

During November, the chaotic wind field effectively mixes the high-latitude perturbed air with lower-latitude unperturbed air. By the end of the month (Plates 4c and 4d), NO_y enhancements are less than 10% and ozone depletions are less than 5%. Perturbed material can be found at all locations outside the tropics. In December, at 10.8 hPa, the summertime circulation becomes established, and the mixing nearly eliminates horizontal gradients of $p(NO_y)$ and $p(O_3)$. By December 31, 1989 (Plates 4e and 4f), contours of $p(NO_y)$ and $p(O_3)$ simply spiral in a circumpolar easterly fashion.

At 10.8 hPa the easterlies at 60°S are strongest (zonal average ~ -15 m s^{-1}) near solstice and begin slowing during January. By early February, analysis of GSMM (and NMC) mean zonal wind easterlies have speeds less than 10 m s^{-1}. At this time the easterly rotation of the contours of $p(NO_y)$ and $p(O_3)$ about the pole is sluggish (Plates 5a and 5b). By February 15, 1990, weak westerlies appear between 60°S and 90°S, and the contours of $p(NO_y)$ and $p(O_3)$ begin circulating cyclonically about the pole. As the vortex begins to slowly spin up, descent begins in its interior. This is reflected in the polar maximum of $p(O_3)$ (Plate 5d), whose zonally averaged maximum lies at pressures just slightly less than 10 hPa. By April 1, 1990, a well-defined polar vortex can be seen in both $p(NO_y)$ and $p(O_3)$ (Plates 5e and 5f). At this time the remaining southern hemisphere ozone perturbation is gently descending through 10.8 hPa. This is discussed in section 6.

Jackman et al. [1993] focused on the hemispheric asymmetries in the evolution of the NO_y and O_3 perturbations during the first two months of the three-dimensional simulation. However, the three-dimensional model used by *Jackman et al.* [1993] did not include chlorine chemistry and predicted a larger decrease (8%) for the southern hemisphere in ozone at 4.18 hPa for the 60° to 80° latitude band by the end of December than was actually observed in NOAA 11 SBUV/2 measurements (1%). The model also predicted a larger ozone decrease (18%) for the northern hemisphere at 4.18 hPa than observed (12%). In the experiments outlined here, however, chlorine chemistry is included. This promotes the production of $ClONO_2$ through

$$ClO + NO_2 + M \rightarrow ClONO_2 + M,$$

decreases the sensitivity of ozone to NO_y, and leads to smaller depletions of ozone. The results are detailed in Table 1.

The improvement seen in the three-dimensional model experiments is thus primarily attributable to their simulation of horizontal mixing and because of the characteristics of the wind fields into which the chemical perturbations are placed. In the northern hemisphere the polar vortex is forming. Perturbed constituents eventually fill the vortex and are prevented from mixing with low- latitude material by vortex dynamics. In the southern hemisphere the vortex is breaking apart. The flow field is characterized by rapid mixing in both meridional and longitudinal extents. Since latitudinally dependent mixing is not parameterized in the two-dimensional model, those calculations did not generate the observed interhemispheric differences.

Table 1. Measurements and Model Predictions of Ozone Depletion in the Latitude Band 60°-80° at 4 hPa

	Southern Hemisphere,%	Northern Hemisphere,%
NOAA 11 SBUV/2 measurements (December 1989 compared to December 1990 and December 1991 average)	-1	-12
Two-dimensional model predictions (with chlorine chemistry)	-20	-21
Three-dimensional model predictions (without chlorine chemistry)	-8	-18
Three-dimensional model predictions (with chlorine chemistry)	-5	-9

5. Temperature Change Associated With October 1989 SPEs

The temperature change associated with SPEs has been discussed in previous studies [e.g., *Reagan et al.*, 1981; *Jackman and McPeters*, 1985; and *Reid et al.*, 1991]. Since ozone is one of the primary radiative absorbing (heating) gases of the middle atmosphere, a decrease in ozone is expected to result in lower temperatures. *Jackman and McPeters* [1985] computed a temperature decrease of a maximum of 1.1°K at 50 km due to the large decreases in ozone observed and computed during the July 13, 1982, SPE. *Reagan et al.* [1981] calculated a temperature decrease of only 2.2°K at 50 km during the much larger August 1972 SPE. *Reid et al.* [1991] compute maximum temperature decreases of about 3-3.5°K between 40 and 45 km at 75°S at the end of October 1989, caused by the October 1989 SPEs.

We have used an off-line computation of temperature changes resulting from the simulated ozone

decreases computed from comparing the "1989-1990 SPE run" to the "1989-1990 base run." The radiation code used has been described by *Rosenfield et al.* [1987], as modified by *Rosenfield* [1991]. Our calculations indicate that much less of a temperature decrease would be expected in the northern hemisphere than in the southern hemisphere in November and December 1989 (the period of maximum ozone decrease from the October 1989 SPEs) because of the difference in Sun angle in the hemispheres at this time. Decreases in the upper stratospheric temperature associated with ozone decreases of 20-25% are computed to be a maximum of about 3°K between 44 and 48 km at 75°S in the southern hemisphere, similar to the results of *Reid et al.* [1991], and a maximum of about 1°K between 40 and 47 km at 61°N in the northern hemisphere.

6. Northern Polar Downward Transport From November 1989 to March 1990

Polar winter downward transport in the middle atmosphere has been observed in satellite measurements [e.g., *Russell et al.*, 1984; *Fisher et al.*, 1993; *Lopez-Valverde et al.*, 1993] and during in situ aircraft sampling missions [*Loewenstein et al.*, 1989, 1990] and has been simulated in three-dimensional tracer experiments [*Nielsen et al.*, 1994] and in trajectory studies [*Fisher et al.*, 1993]. Such wintertime downward transport has also been simulated in two-dimensional model studies of SPE-effects on the stratosphere (see *Jackman et al.*, 1990, Figure 10; *Reid et al.*, 1991, Figure 4] (Figure 2, this study).

As noted above, some two-dimensional modeling studies indicate downward transport during the wintertime. Our three-dimensional model predicts a slightly larger downward motion during the 1989-1990 northern winter, which is illustrated in Plates 6 and 7. The SPE initiates substantial production of NO_y (Plate 6a) in the mesosphere and upper stratosphere. In fact, the ion pair production from the October 1989 SPEs influence virtually the entire stratosphere. The slightly larger values for $p(NO_y)$ in the northern hemisphere reflect the smaller ambient NO_y mixing ratios in the base data set. Plate 6b shows that the initial condition assumes no ozone depletion. That is, the ozone perturbation is derived and therefore does not appear on the zeroth time step. Sunlight promotes a steady loss of NO_y, especially at pressures less than 1 hPa, so the NO_y perturbation is somewhat more quickly quenched over the southern polar region. The effect is noticeable after only a few days (Plate 6c). Plate 6e, 7a, 7c, and 7e illustrate the continued descent of NO_y in the northern polar regions. The NO_y enhancement (with a peak above 4 hPa) is moved to ~30-40 hPa over the course of 5 months (Plate 7e).

The transport of southern mesospheric polar NO_y to the northern mesospheric regions is best illustrated by Plates 7a, 7c, and 7e. Meridional transport is fast in the mesosphere and communication of the two hemispheres does take place over a few months time period in our model simulations.

The maximum O_3 decrease does not always correspond to the maximum NO_y increase because of the importance of the loss of ozone to the different families (O_x, NO_y, HO_x, Cl_y) in different regions of the middle atmosphere [e.g., *Crutzen and Schmailzl*, 1983; *Jackman et al.*, 1986]. In the mesosphere (above ~1 hPa) the HO_x loss processes dominate; in the upper stratosphere (~5 to 1 hPa) all families contribute to ozone loss; and in the middle stratosphere (~30 to 5 hPa) the NO_y family dominates the ozone loss. Because of these reasons (1) the maximum NO_y increase on November 5, 1989 (see Plates 6c and 6d), which peaks in the mesosphere in both hemispheres does not correspond to the maximum O_3 decrease which peaks in the upper stratosphere; and (2) the maximum NO_y increase on March 31, 1990 (see Plates 7e and 7f) which peaks in the upper stratosphere in the southern hemisphere does not correspond to the maximum O_3 decrease which peaks in the middle stratosphere.

Which of these modeling simulations (two-dimensional or three-dimensional) of downward transport is closer to measurements in the 1989-1990 northern winter? Fortunately, during this time period the SAGE II instrument was taking measurements of NO_2 and O_3. Before we present comparisons of model-simulated changes in NO_2 and O_3 to SAGE II measurements, we first show comparisons of absolute amounts of these two constituents in Figure 4 for March 31, 1990. The SAGE II measurements are taken at sunset. This especially affects the model/measurement comparison to NO_2, which has a strong diurnal cycle (see discussion by *Prather and Remsberg* [1993]). Our three-dimensional model comparisons are taken from a "near sunset" condition, whereas our two-dimensional model comparisons are all from a "daytime average" calculation. The model simulations are within about 25% of the peak value of NO_2 in the middle stratosphere between 30 and 35 km. In the lower stratosphere the "gas phase only" two-dimensional model simulation appears to be in better agreement with the SAGE II data than the "gas phase + het" two-dimensional model simulation. However, the "gas phase only" three-dimensional simulation overpredicts the amount of NO_2.

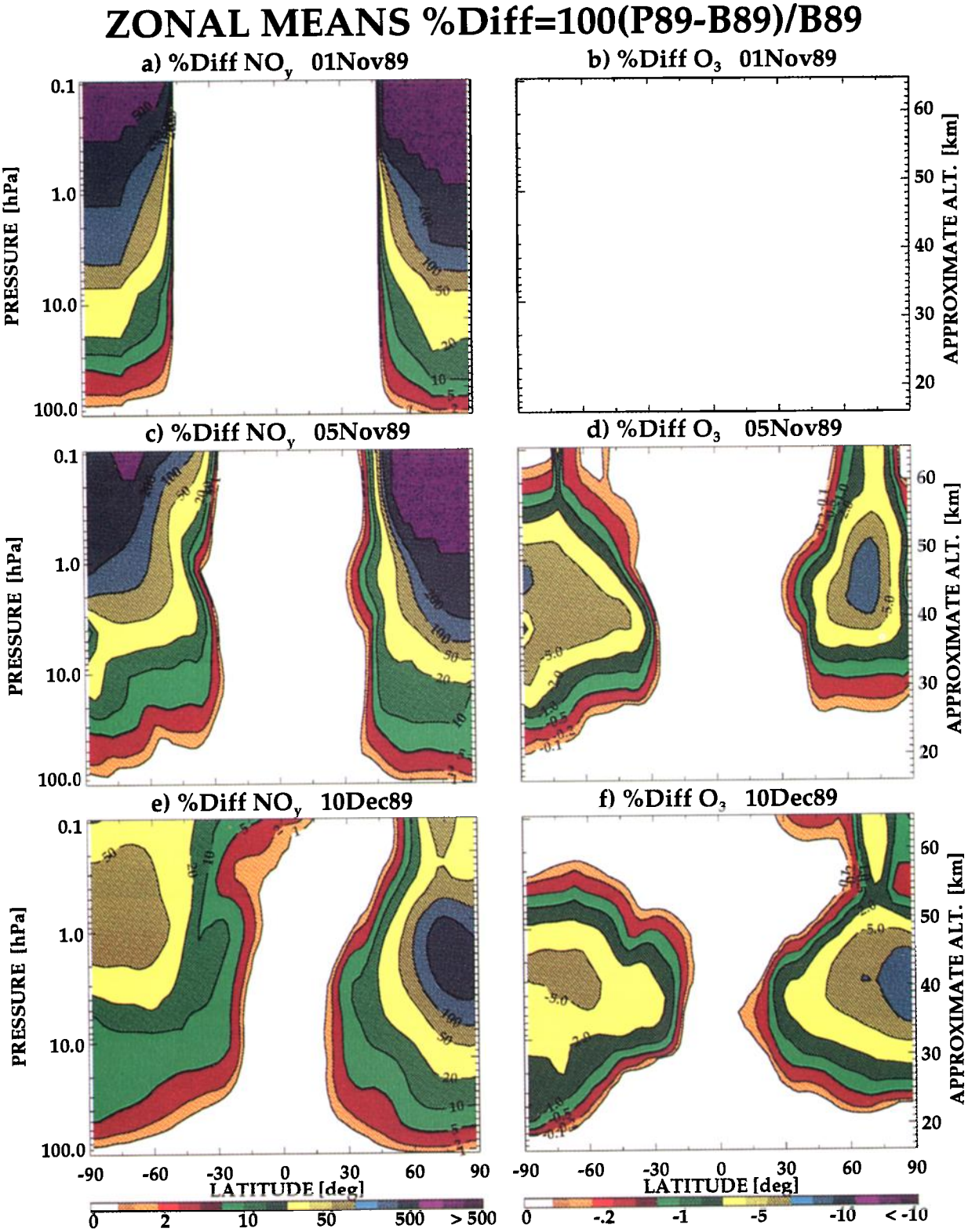

Plate 6. (a, c, and e) Zonal mean model prediction of NO_y and (b, d, and f) O_3 percentage change predicted from the GSFC three-dimensional model for November 1, 1989, November 5, 1989, and December 10, 1989. The percentage difference (%diff) is computed by subtracting the "1989-1990 base run" (B89) from the "1989-1990 SPE run" (P89), dividing that difference by the "1989-1990 base run" (B89), and multiplying the result by 100.

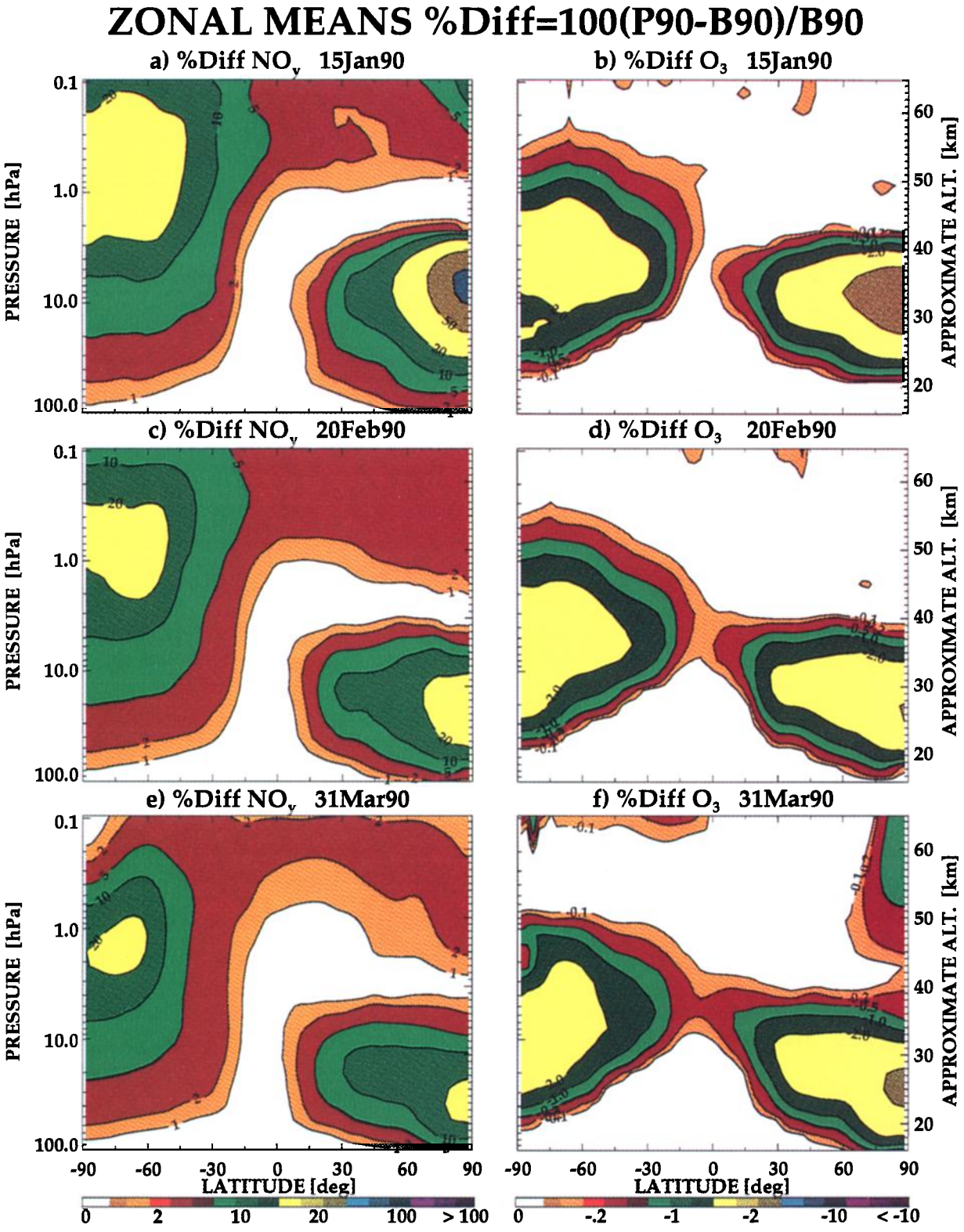

Plate 7. (a, c, and e) Zonal mean model prediction of NO_y and (b, d, and f) O_3 percentage change predicted from the GSFC three-dimensional model for January 15, 1990, February 20, 1990, and March 31, 1990. The percentage difference (%diff) is computed by subtracting the "1989-1990 base run" (B90) from the "1989-1990 SPE run" (P90), dividing that difference by the "1989-1990 base run" (B90), and multiplying the result by 100.

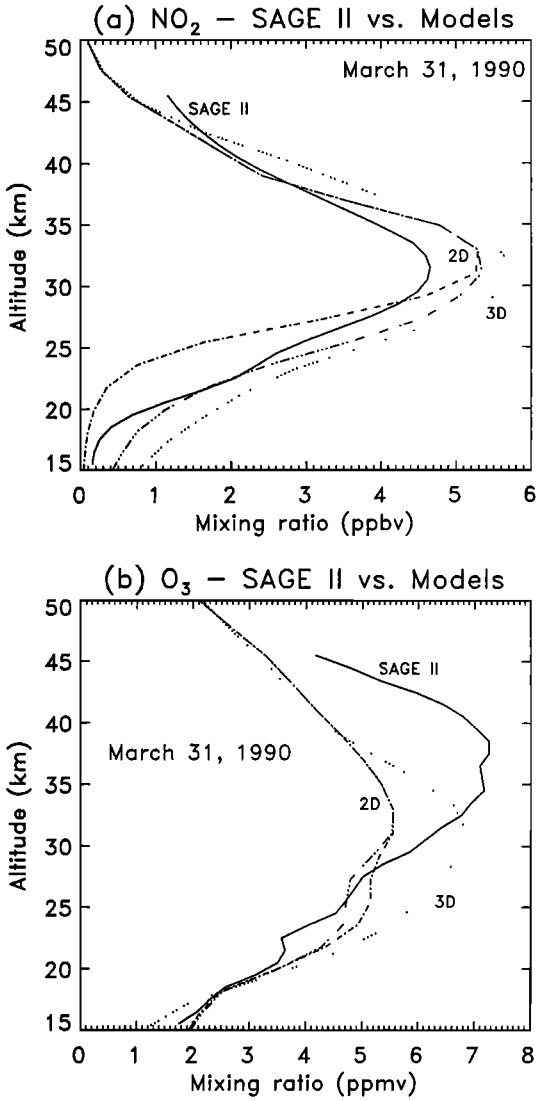

Figure 4. GSFC two-dimensional and three-dimensional model zonal mean predictions for (a) NO_2 and (b) O_3 compared to SAGE II zonal mean measurements (solid curve) for March 31, 1990, at 70°N. The GSFC two-dimensional "gas phase + het" and "gas phase only" results are given by the dashed-dotted and dashed-dotted-dotted-dottedcurves, respectively. The three-dimensional model predictions (dotted curve) were taken from the "1989-1990 SPE run."

None of the models simulate the SAGE II O_3 peak between about 34 and 38 km very well, a problem for most models [see *Prather and Remsberg*, 1993]. The O_3 in the lowest part of the stratosphere is reasonably well represented by the models, however, the two-dimensional models predict larger amounts of O_3 between about 20 and 25 km than observed in SAGE II measurements, and the three-dimensional model predicts larger amounts of O_3 between about 20 and 32 km than observed in the SAGE II measurements.

We are unable to resolve the outstanding model-measurement discrepancies pointed out by *Prather and Remsberg* [1993] in this study. We thus turn to a calculation of relative percentage changes between SAGE II measurements in 1990 and 1987 and compare that with a suite of model simulations over for the remainder of this paper. The NO_2 and O_3 changes due to the October 1989 SPEs were estimated by computing the SAGE II measured differences

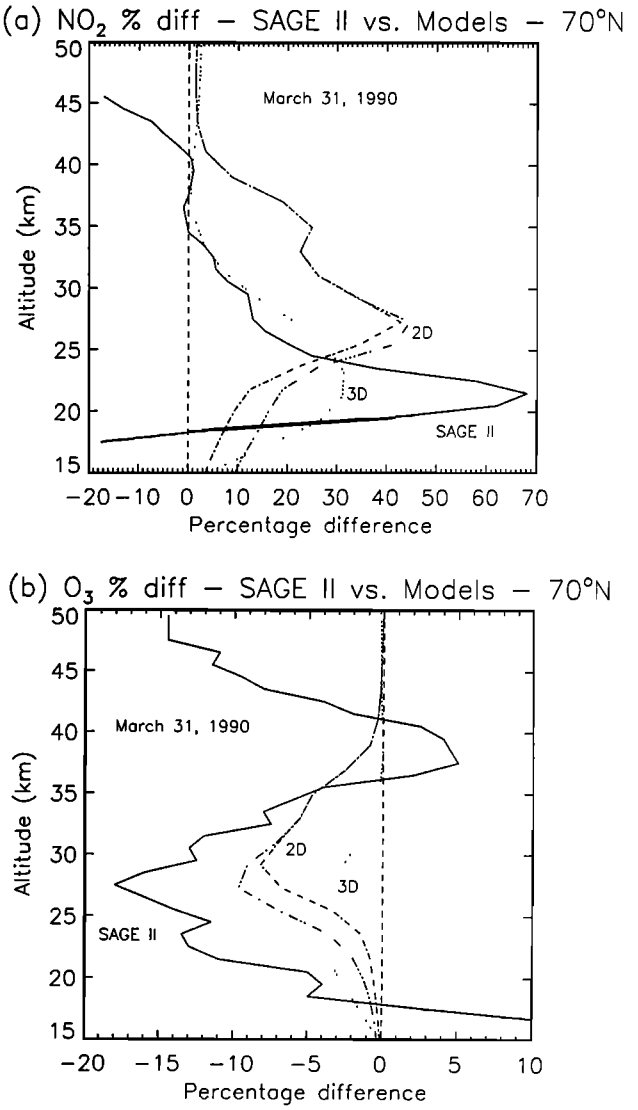

Figure 5. GSFC two-dimensional and three-dimensional model zonal mean predictions for (a) NO_2 and (b) O_3 percentage change compared to SAGE II zonal mean measurements (solid curve) for March 31, 1990, at 70°N. The GSFC two-dimensional "gas phase + het" and "gas phase only" results are given by the dashed-dotted and dashed-dotted-dotted-dotted curves, respectively. The three-dimensional model predictions (dotted curve) were taken from a comparison of the "1989-1990 SPE run" to the "1989-1990 base run."

between 1990 and 1987 using data that was averaged over a 10-day period centered on March 31. The SAGE II zonal mean changes in NO_2 and O_3 at 70°N for March 31, 1990, compared to March 31, 1987, are represented by the solid curves in Figure 5. Measurements in 1990 were compared to those in 1987 rather than 1988 or 1989 because of the substantial differences in atmospheric constituents which result from being in different phases of the quasi-biennial oscillation (QBO): 1990 and 1987 are in the easterly phase of the QBO [see *Hasebe*, 1994, Figure 2].

The two-dimensional model results (both "gas phase only" and "gas phase + het") show significant NO_2 enhancement on March 31, 1990, at 70°N due to the October 1989 SPEs (Figure 5a), but the peak is near 27 km, several kilometers higher than that indicated in the SAGE II data. Surprisingly, the ozone decreases predicted by the two separate two-dimensional model modes (Figure 5b) are in better agreement with the SAGE II data, both showing peak decreases between 25 and 30 km. The double-peaked shape of the NO_2 change comes from the initial source function of NO_x produced by the SPEs. The three-dimensional model zonally averaged value at 70°N (Figure 5a) shows NO_2 enhancement at a lower altitude from that of the two-dimensional model, in better agreement with SAGE II; however, the magnitude of the NO_2 increase (~31%) is less than measured (~68%). The three-dimensional model predicted ozone decrease (~4%) is substantially less than measured by SAGE II (~18%).

Since our mechanistic model is forced to simulate the desired time period (in this case November 1, 1989, to April 2, 1990), it was expected that the three-dimensional model would simulate not only the altitude of maximum NO_2 enhancement but also the magnitude much better than the two-dimensional "climatological" model. This was not quite the case, however, as can be observed in Figure 5.

As explained above, the SAGE II results were derived by comparing measurements in year 1990 with 1987. If there are substantial interannual differences between 1990 and 1987 (notwithstanding the fact that both years are in the same phase of the QBO), then differences might be expected in the two years, even if there were no large SPEs in late 1989. Because of this we compare our "1986-1987 base run" case to the "1989-1990 SPE run" as well.

We present the NO_2 changes for the "1989-1990 SPE run" versus the "1989-1990 base run" in Figure 6a and the "1989-1990 SPE run" versus the "1986-1987 base run" in Figure 6b for March 31st. Therefore the NO_2 change in Figure 6b has contributions from both the SPEs and interannual variability. Increases in NO_2 of over 40% are evident in Figure 6a at high latitudes (>78°N) and low altitudes (28-52 hPa). Even larger NO_2 increases are predicted and illustrated in Figure 6b. This figure shows NO_2 enhancements of over 140% for latitudes >78°N and altitudes from 30 to 80 hPa. A sharp gradient with latitude and altitude is also apparent. Decreases in

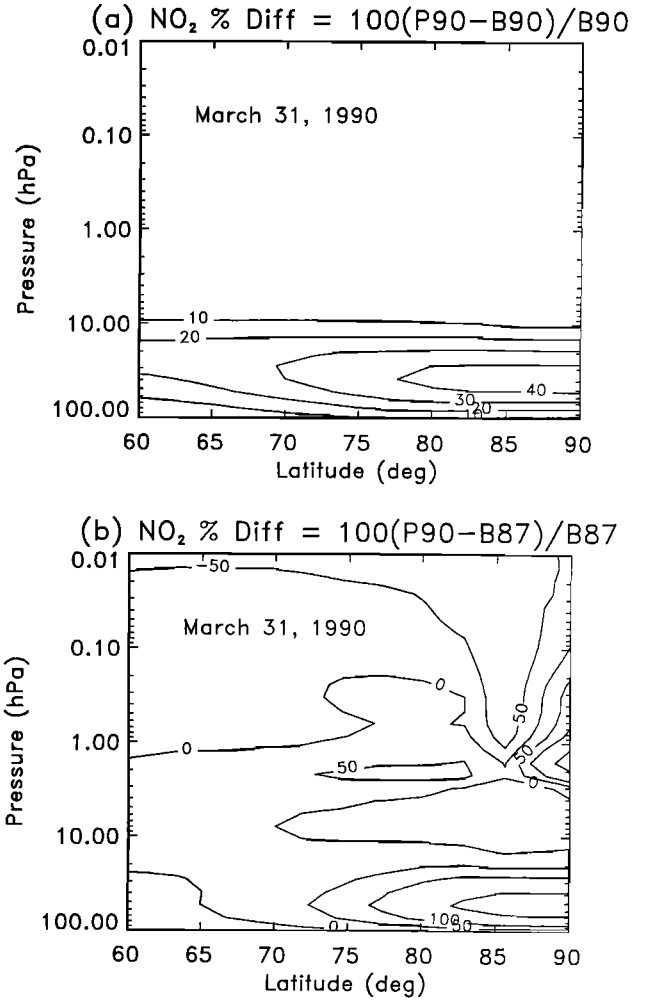

Figure 6. GSFC three-dimensional model zonal mean predictions for NO_2 percentage change on March 31, 1990, from 60° to 90°N for two separate model comparisons. (a) The percentage difference (NO_2 % diff) is computed by subtracting the "1989-1990 base run" (B90) from the "1989-1990 SPE run" (P90), dividing that difference by the "1989-1990 base run" (B90), and multiplying the result by 100. Contour levels plotted are 10, 20, 30, and 40%. (b) The percentage difference (NO_2 % diff) is computed by subtracting the "1986-1987 base run" (B87) from the "1989-1990 SPE run" (P90), dividing that difference by the "1986-1987 base run" (B87), and multiplying the result by 100. Contour levels plotted are -50, 0, 50, 100, and 200%.

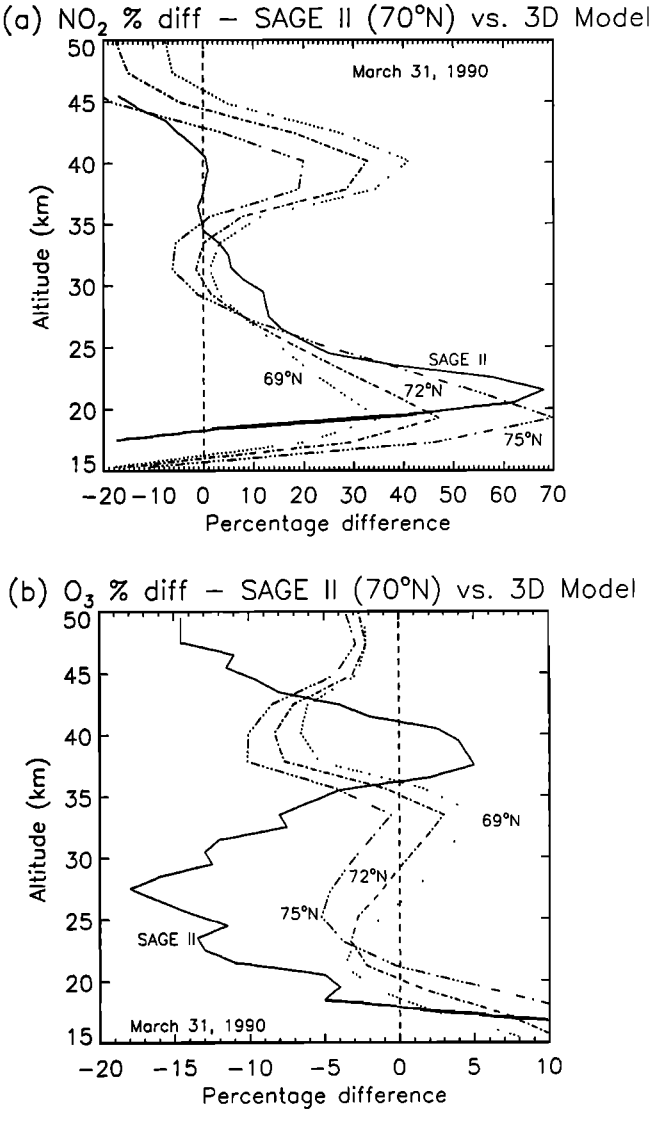

Figure 7. GSFC three-dimensional model zonal mean predictions for the "1989-1990 SPE run" compared to the "1986-1987 base run" at 69°N (dotted curve), 72°N (dashed-dotted curve), and 75°N (dashed-dotted-dotted-dotted curve) for (a) NO_2 and (b) O_3 percentage change compared to SAGE II measurements at 70°N for March 31, 1990 (solid curve).

NO_2 are even predicted in certain regions of the middle and upper stratosphere in Figure 6b. The NO_2 change due to the SPEs is obscured by the NO_2 change due to interannual variability at the very highest latitudes. Clearly, we need to compare the difference between the "1989-1990 SPE run" and the "1986-1987 base run" with measurements.

We show our NO_2 and O_3 percentage differences for the "1989-1990 SPE run" compared to the "1986-1987 base run" along with the SAGE II measured changes in Figure 7. We include three separate latitudes (69°, 72°, and 75°N) in this comparison because of the very sharp predicted latitudinal gradient. Figure 7a illustrates that the very large observed "sharply peaked" enhancements in NO_2 in the lower stratosphere at 70°N can be simulated assuming that there are uncertainties of a few degrees in latitude in the stratospheric meteorological patterns forced by the NMC geopotentials at 100 hPa.

The NO_2 and O_3 changes observed in SAGE II in the middle and upper stratosphere are not so well represented in our three-dimensional simulation. We show a dynamically driven NO_2 increase at about 40 km which forces an O_3 decrease in the same region. The SAGE II measurements show nearly no NO_2 change and a small O_3 increase at the same altitude. Our model simulation more closely resembles the evolution of the observed planetary wave structure near 100 hPa (our lower boundary) and at lower pressures the evolution is more likely to deviate from the observed. After 5 months of simulation there does appear to be a phase error that increases with height.

Analysis of our three-dimensional studies indicates that the SAGE II NO_2 measured 68% increase at 70°N between 1987 and 1990 has contributions from both SPEs and interannual variability. The SPEs may account for about half of the SAGE II measured changes and the more persistent downward transport in the 1989-1990 winter compared to the 1986-1987 winter may account for the other half.

Our simulation for ozone changes on March 31, 1990, caused by interannual and SPE forcings have several problems. The magnitude of the ozone depletion in the middle to lower stratosphere is underpredicted and the SAGE II ozone increase observed between 36 and 41 km is not predicted in our three-dimensional model. Ozone is influenced by other factors than NO_2 and interannual dynamical changes, thus its quantitative variations from one year to another are much more difficult to simulate. Inclusion of heterogeneous chemistry on polar stratospheric clouds in our model simulations would probably lead to better agreement between our predictions and measurements. The northern hemisphere polar winter lower stratosphere was much colder in 1990 than that in 1987, making it more conducive for polar stratospheric cloud formation [*Cerniglia et al.*, 1994] and ozone depletion.

7. Conclusions

Substantial middle atmospheric effects have been simulated and measured to be associated with the October 1989 SPEs. NO_x constituents NO and NO_2 have been measured by both rockets and satellite

(SAGE II) to be increased as a result of these SPEs. The rocket-measured NO increase during the October 1989 SPEs is fairly well simulated. About half of the increase in NO_2 measured by SAGE II near the end of March 1990 (when compared to the end of March 1987) is computed to be caused by the October 1989 SPEs. The other half of the NO_2 enhancement near the end of March 1990 is probably caused by the interannual dynamical differences between 1990 and 1987.

Ozone decreases measured by the SBUV/2 instrument in December 1989 in the upper stratosphere northern hemisphere are caused by the October 1989 SPEs. Large interhemispheric differences in ozone depletions observed by SBUV/2 near 4 hPa are caused by the different polar dynamical conditions in the November-December 1989 time period. Maximum temperature decreases driven by our simulated ozone decrease in the upper stratosphere are about 3°K near 75°S and about 1°K near 61°N.

The ozone depletions observed by SAGE II near the end of March 1990 in the lower northern stratosphere may be more greatly affected by differences between the winters of 1986-1987 and 1989-1990 than by the solar proton events. Colder polar stratospheric temperatures in the 1989-1990 winter compared to the 1986-1987 winter could have led to a larger ozone depletion in the 1989-1990 winter because of heterogeneous processes and need to be investigated further.

Acknowledgments. The authors would like to thank Thomas P. Armstrong and Claude M. Laird (both at the University of Kansas) for sending solar proton data that were used in the ion pair production computations for this paper. We also thank Walt Planet and NOAA/NESDIS for furnishing data from the NOAA 11 SBUV/2. Funds for computations were provided by the EOS project. We acknowledge NASA Headquarters Atmospheric Chemistry Modeling and Analysis Program for support during the time that this project was undertaken. Finally, we thank two anonymous reviewers for constructive comments on this manuscript. This is contribution number 77 from the Stratospheric General Circulation With Chemistry Project.

References

Allen, D. J., A. R. Douglass, R. B. Rood, and P. D. Guthrie, Application of a monotonic upstream-biased transport scheme to three-dimensional constituent transport calculations, *Mon. Weather Rev.*, *119*, 2456-2464, 1991.

Armstrong, T. P., C. Brundardt, and J. E. Meyer, Satellite observations of interplanetary and polar cap solar particle fluxes from 1963 to the present, in *Weather and Climate Response to Solar Variations*, edited by B. M. McCormac, pp. 71-79, Colorado Associated University Press, Boulder, 1983.

Cerniglia, M. C., C. H. Jackman, J. E. Nielsen, and A. R. Douglass, Interannual differences of the 1986/87 and 1989/90 Northern Hemisphere stratospheric winters, *EOS Trans. AGU*, *75* (16), 100, 1994.

Crutzen, P. J., and U. Schmailzl, Chemical budgets of the stratosphere, *Planet. Space Sci.*, *31*, 1009-1032, 1983.

Crutzen, P. J., I. S. A. Isaksen, and G. C. Reid, Solar proton events: Stratospheric sources of nitric oxide, *Science*, *189*, 457-458, 1975.

DeMore, W. B., S. P. Sander, D. M. Golden, M. J. Molina, R. F. Hampson, M. J. Kurylo, C. J. Howard, and A. R. Ravishankara, Chemical kinetics and photochemical data for use in stratospheric modeling, *JPL Publ. 90-1*, 217 pp., 1990.

Douglass, A. R., C. H. Jackman, and R. S. Stolarski, Comparison of model results transporting the odd nitrogen family with results transporting separate odd nitrogen species, *J. Geophys. Res.*, *94*, 9862-9872, 1989.

Fisher, M., A. O'Neill, and R. Sutton, Rapid descent of mesospheric air into the stratospheric polar vortex, *Geophys. Res. Lett.*, *20*, 1267-1270, 1993.

Fleming, E. L., S. Chandra, C. H. Jackman, D. B. Considine, and A. R. Douglass, The middle atmospheric response to short and long term solar UV variations: Analysis of observations and two-dimensional model results, *J. Atmos. Terr. Phys.*, *57*, 333-365, 1995.

Hasebe, F., Quasi-biennial oscillations of ozone and diabatic circulation in the equatorial stratosphere, *J. Atmos. Sci.*, *51*, 729-745, 1994.

Heath, D. F., A. J. Krueger, and P. J. Crutzen, Solar proton event: Influence on stratospheric ozone, *Science*, *197*, 886-889, 1977.

Jackman, C. H., Energetic particle influences on NO_y and ozone in the middle atmosphere, *Geophys. Monogr. 75*, *IUGG*, *15*, 131-139, 1993.

Jackman, C. H., and R. D. McPeters, The response of ozone to solar proton events during solar cycle 21: A theoretical interpretation, *J. Geophys. Res.*, *90*, 7955-7966, 1985.

Jackman, C. H., J. E. Frederick, and R. S. Stolarski, Production of odd nitrogen in the stratosphere and mesosphere: An intercomparison of source strengths, *J. Geophys. Res.*, *85*, 7495-7505, 1980.

Jackman, C. H., and R. D. McPeters, The response of ozone to solar proton events during solar cycle 21: A theoretical interpretation, *J. Geophys. Res.*, *90*, 7955-7966, 1985.

Jackman, C. H., R. S. Stolarski, and J. A. Kaye, Two-dimensional monthly average ozone balance from limb infrared monitor of the stratosphere and stratospheric and mesospheric sounder data, *J. Geophys. Res.*, *91*, 1103-1116, 1986.

Jackman, C. H., P. D. Guthrie, and J. A. Kaye, An intercomparison of nitrogen-containing species in Nimbus 7 LIMS and SAMS data, *J. Geophys. Res.*, *92*, 995-1008, 1987.

Jackman, C. H., A. R. Douglass, R. B. Rood, R. D. McPeters, and P. E. Meade, Effect of solar proton events on the middle atmosphere during the past two solar cycles as computed using a two-dimensional model, *J. Geophys. Res.*, *95*, 7417-7428, 1990.

Jackman, C. H., A. R. Douglass, K. F. Brueske, and S. A. Klein, The influence of dynamics on two-dimensional

model results: Simulations of ^{14}C and stratospheric aircraft NO_x injections, *J. Geophys. Res.*, *96*, 22,559-22,572, 1991.

Jackman, C. H., J. E. Nielsen, D. J. Allen, M. C. Cerniglia, R. D. McPeters, A. R. Douglass, and R. B. Rood, The effects of the October 1989 solar proton events on the stratosphere as computed using a three-dimensional model, *Geophys. Res. Lett.*, *20*, 459-462, 1993.

Lary, D. J., M. P. Chipperfield, J. A. Pyle, W. A. Norton, and L. P. Riishojgaard, Three dimensional tracer initialization and general diagnostics using equivalent PV latitude - potential temperature coordinates, *Q. J. R. Meteorol. Soc.*, *121*, 187-210, 1994.

Loewenstein, M. J., J. R. Podolske, K. R. Chan, and S. E. Strahan, Nitrous oxide as a dynamical tracer in the 1987 Airborne Antarctic Ozone Experiment, *J. Geophys. Res.*, *94*, 11,589-11,598, 1989.

Loewenstein, M. J., J. R. Podolske, K. R. Chan, and S. E. Strahan, N_2O as a dynamical tracer in the Arctic vortex, *Geophys. Res. Lett.*, *17*, 477-480, 1990.

Lopez-Valverde, M. A., M. Lopez-Puertas, C. J. Marks, and F. W. Taylor, Global and seasonal variations in middle atmosphere CO from UARS/ISAMS, *Geophys. Res. Lett.*, *20*, 1247-1250, 1993.

McPeters, R. D., and C. H. Jackman, The response of ozone to solar proton events during solar cycle 21: The observations, *J. Geophys. Res.*, *90*, 7945-7954, 1985.

McPeters, R. D., C. H. Jackman, and E. G. Stassinopoulos, Observations of ozone depletion associated with solar proton events, *J. Geophys. Res.*, *86*, 12,071-12,081, 1981.

Nielsen, J. E., R. B. Rood, A. R. Douglass, M. C. Cerniglia, D. J. Allen, and J. E. Rosenfield, Tracer evolution in winds generated by a global spectral mechanistic model, *J. Geophys. Res.*, *99*, 5399-5420, 1994.

Porter, H. S., C. H. Jackman, and A. E. S. Green, Efficiencies for production of atomic nitrogen and oxygen by relativistic proton impact in air, *J. Chem. Phys.*, *65*, 154-167, 1976.

Prather, M. J., and E. E. Remsberg, The atmospheric effects of stratospheric aircraft: Report of the 1992 models and measurements workshop, *NASA Ref. Publ. 1292*, 1993.

Reagan, J. B., R. E. Meyerott, R. W. Nightingale, R. C. Gunton, R. G. Johnson, J. E. Evans, W. L. Imhof, D. F. Heath, and A. J. Krueger, Effects of the August 1972 solar particle events on stratospheric ozone, *J. Geophys. Res.*, *86*, 1473-1494, 1981.

Reid, G. C., S. Solomon, and R. R. Garcia, Response of the middle atmosphere to the solar proton events of August-December, 1989, *Geophys. Res. Lett.*, *18*, 1019-1022, 1991.

Rood, R. B., J. E. Nielsen, R. S. Stolarski, A. R. Douglass, J. A. Kaye, and D. J. Allen, Episodic total ozone minima and associated effects on heterogeneous chemistry and lower stratospheric transport, *J. Geophys. Res.*, *97*, 7979-7996, 1992.

Rosenfield, J. E., A simple parameterization of ozone infrared absorption for atmospheric heating rate calculations, *J. Geophys. Res.*, *96*, 9065-9074, 1991.

Rosenfield, J. E., M. R. Schoeberl, and M. A. Geller, A computation of the stratospheric diabatic circulation using an accurate radiative transfer model, *J. Atmos. Sci.*, *44*, 859-876, 1987.

Rusch, D. W., J.-C. Gerard, S. Solomon, P. J. Crutzen and G. C. Reid, The effect of particle precipitation events on the neutral and ion chemistry of the middle atmosphere, 1, Odd nitrogen, *Planet. Space Sci.*, *29*, 767-774, 1981.

Russell, J. M., III, S. Solomon, L. L. Gordley, E. E. Remsberg, and L. B. Callis, The variability of stratospheric and mesospheric NO_2 in the polar winter night observed by LIMS, *J. Geophys. Res.*, *89*, 7267-7275, 1984.

Solomon, S., and P. J. Crutzen, Analysis of the August 1972 solar proton event including chlorine chemistry, *J. Geophys. Res.*, *86*, 1140-1146, 1981.

Solomon, S., D. W. Rusch, J.-C. Gerard, G. C. Reid, and P. J. Crutzen, The effect of particle precipitation events on the neutral and ion chemistry of the middle atmosphere, 2, Odd hydrogen, *Planet. Space Sci.*, *29*, 885-892, 1981.

Solomon, S., G. C. Reid, D. W. Rusch, and R. J. Thomas, Mesospheric ozone depletion during solar proton events, paper presented at the Sixth ESA-PAC Meeting, Eur. Space Agency, Interlaken, Switzerland, April 12-19, 1983.

Thomas, R. J., C. A. Barth, G. J. Rottman, D. W. Rusch, G. H. Mount, G. M. Lawrence, R. W. Sanders, G. E. Thomas, and L. E. Clemens, Mesospheric ozone depletion during the solar proton event of July 13, 1982, 1, Measurement, *Geophys. Res. Lett.*, *10*, 253-255, 1983.

Weeks, L. H., R. S. CuiKay, and J. R. Corbin, Ozone measurements in the mesosphere during the solar proton event of November 2, 1969, *J. Atmos. Sci.*, *29*, 1138-1142, 1972.

Weisenstein, D., M. K. W. Ko, J. M. Rodriguez, and N. D. Sze, Impact of heterogeneous chemistry on model-calculated ozone change due to HSCT aircraft, *Geophys. Res. Lett.*, *18*, 1991-1994, 1991.

World Meteorological Organization (WMO), Scientific assessment of ozone depletion: 1991, *WMO Global Ozone Res. and Monit. Proj. Rep. 25*, 1992.

Zadorozhny, A. M., G. A. Tuchkov, V. N. Kikhtenko, J. Lastovicka, J. Boska, and A. Novak, Nitric oxide and lower ionosphere quantities during solar particle events of October 1989 after rocket and ground-based measurements, *J. Atmos. Terr. Phys.*, *54*, 183-192, 1992.

D. J. Allen, M. C. Cerniglia, J. E. Nielsen, and J. E. Rosenfield, Applied Research Corporation, Landover, MD 20785. (e-mail: allen@twod.gsfc.nasa.gov; mcc@aurora.gsfc.nasa.gov; nielsen@twod.gsfc.nasa.gov; rose@euterpe.gsfc.nasa.gov).

A. R. Douglass, C. H. Jackman (corresponding author), R. D. McPeters, and R. B. Rood, Laboratory for Atmospheres, NASA Goddard Space Flight Center, Greenbelt, MD 20771. (e-mail: douglass@persephone.gsfc.nasa.gov; jackman@assess.gsfc.nasa.gov; mcpeters@wrabbit.gsfc.nasa.gov; rood@dao.gsfc.nasa.gov)

J. M. Zawodny, Atmospheric Sciences Division, NASA Langley Research Center, Hampton, VA 23665. (e-mail: zawodny@arbd0.larc.nasa.gov)

(Received October 4, 1994; revised January 14, 1995; accepted January 14, 1995.)